Perforation of the Tunnel Wall in Carbamoyl Phosphate Synthetase Derails the Passage of Ammonia between Sequential Active Sites†

Jungwook Kim and Frank M. Raushel*

Department of Chemistry, Texas A&M University, P.O. Box 30012, College Station, Texas 77842-3012

Received January 7, 2004; Revised Manuscript Received March 9, 2004

ABSTRACT: Carbamoyl phosphate synthetase (CPS) from *Escherichia coli* consists of a small subunit (∼42 kDa) and a large subunit (∼118 kDa) and catalyzes the biosynthesis of carbamoyl phosphate from MgATP, bicarbonate, and glutamine. The enzyme is able to utilize external ammonia as an alternative nitrogen source when glutamine is absent. CPS contains an internal molecular tunnel, which has been proposed to facilitate the translocation of reaction intermediates from one active site to another. Ammonia, the product from the hydrolysis of glutamine in the small subunit, is apparently transported to the next active site in the large subunit of CPS over a distance of about 45 Å. The ammonia tunnel that connects these two active sites provides a direct path for the guided diffusion of ammonia and protection from protonation. Molecular damage to the ammonia tunnel was conducted in an attempt to induce leakage of ammonia directly to the protein exterior by the creation of a perforation in the tunnel wall. A hole in the tunnel wall was made by mutation of integral amino acid residues with alanine residues. The triple mutant αP360A/αH361A/βR265A was unable to utilize glutamine for the synthesis of carbamoyl phosphate. However, the mutant enzyme retained full catalytic activity when external ammonia was used as the nitrogen source. The synchronization of the partial reactions occurring at the three active sites observed with the wild-type CPS was seriously disrupted with the mutant enzyme when glutamine was used as a nitrogen source. Overall, the catalytic constants of the mutant were consistent with the model where the channeling of ammonia has been disrupted due to the leakage from the ammonia tunnel to the protein exterior.

Carbamoyl phosphate synthetase (CPS)[1] catalyzes the formation of carbamoyl phosphate (eq 1), which functions

$$2\text{MgATP} + \text{HCO}_3^- + \text{glutamine} \rightarrow 2\text{MgADP} + \text{glutamate} + \text{P}_i + \text{carbamoyl-P} \quad (1)$$

as the initial building block in the biosynthesis of pyrimidine nucleotides and arginine (*1*). CPS is a heterodimeric enzyme (αβ) composed of small and large subunits of molecular masses 42 and 118 kDa, respectively (Figure 1). The small subunit contains the active site for the hydrolysis of glutamine while the large subunit contains two separate ATP binding sites where the phosphorylation of bicarbonate and carbamate occurs.

CPS also catalyzes the three partial reactions shown in eqs 2−4 (*2*). In the absence of a nitrogen source, CPS

$$\text{glutamine} + \text{H}_2\text{O} \rightarrow \text{glutamate} + \text{NH}_3 \quad (2)$$

$$\text{MgATP} + \text{H}_2\text{O} \rightarrow \text{MgADP} + \text{P}_i \quad (3)$$

$$\text{MgADP} + \text{carbamoyl-P} \rightarrow \text{MgATP} + \text{NH}_2\text{CO}_2^- \quad (4)$$

catalyzes a bicarbonate-dependent ATPase reaction, where bicarbonate is phosphorylated by ATP at the active site located in the N-terminal synthetase domain of the large subunit. The unstable product, carboxy phosphate, is then hydrolyzed by water to yield phosphate and bicarbonate. When glutamine or ammonia is present, carboxy phosphate reacts with ammonia to produce carbamate and phosphate. The carbamate intermediate is phosphorylated by the ATP bound to the C-terminal domain of the large subunit to generate the final product, carbamoyl phosphate. Therefore, two molecules of ADP are formed per every turnover when a nitrogen source is provided. In wild-type CPS, the net rate of ADP formation is accelerated by about an order of magnitude when glutamine or ammonia is present. The partial ATP synthesis reaction from carbamoyl phosphate and ADP occurs at the carbamoyl phosphate binding site in the C-terminal domain of the large subunit. This reaction is essentially the reverse of the last phosphorylation step during the formation of carbamoyl phosphate. The generally accepted reaction mechanism for CPS is summarized in Scheme 1.

The X-ray crystal structure of CPS unveiled the existence of a molecular tunnel for the transport of reaction intermediates between remotely located active sites (*3*). Ammonia is an intermediate during the biosynthesis of carbamoyl phosphate, which is produced upon the hydrolysis of glutamine in the small subunit of the enzyme. The intermediate is delivered to the next active site in the large subunit, which

† This work was supported in part by the NIH (DK 30343) and the Robert A. Welch Foundation (A-840).

* To whom correspondence may be addressed (phone, 979-845-3373; fax, 979-845-9452; e-mail, raushel@tamu.edu).

[1] Abbreviations: CPS, carbamoyl phosphate synthetase; OTCase, ornithine transcarbamoylase, APAD, 3-acetylpyridine adenine dinucleotide; PRTase, phosphoribosylpyrophosphate amidotransferase.

10.1021/bi049945+ CCC: $27.50 © 2004 American Chemical Society
Published on Web 04/17/2004

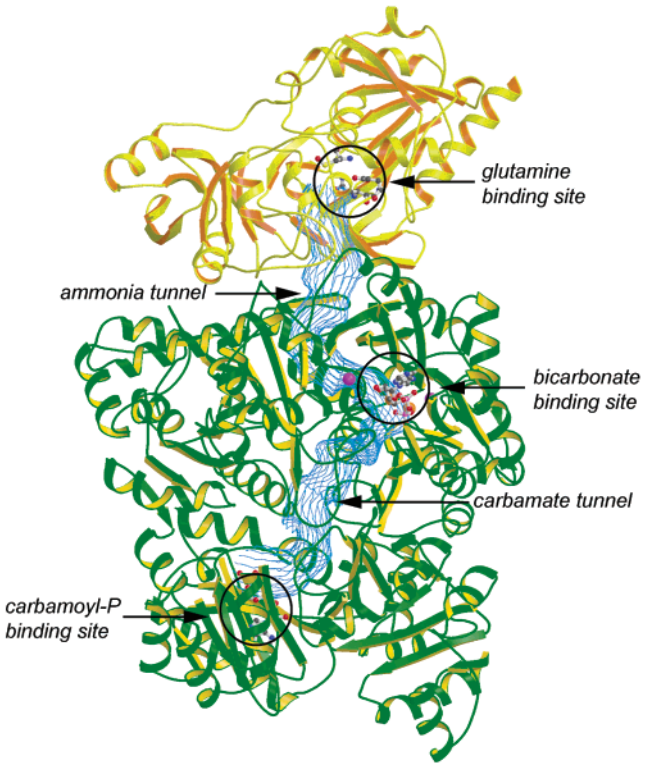

FIGURE 1: Ribbon representation of the three-dimensional structure of CPS from *E. coli*. The three active sites are indicated by the black circles. The ammonia and the carbamate tunnel are displayed in blue. The small subunit is presented in yellow, and the large subunit is displayed in green. The coordinate file for this structure was obtained from Thoden et al. (*3*).

Scheme 1

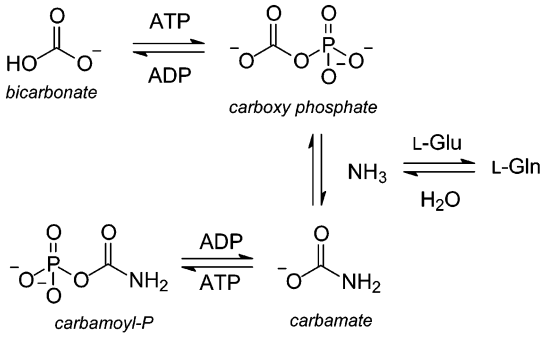

is about 45 Å away from the site of glutamine hydrolysis. The direct channeling of ammonia has been experimentally supported by measuring the competition between the ammonia derived from the hydrolysis of glutamine and exogenous $^{15}NH_3$ added to the bulk solvent (*4*). The preferential incorporation of the ammonia derived from glutamine is consistent with a mechanism where the internally produced ammonia is transferred directly through a molecular tunnel, rather than through a dissociation−reassociation mechanism.

Confirmatory evidence for the direct diffusion of ammonia through a molecular tunnel within CPS was achieved by measurement of the kinetic properties of channeling-impaired mutant enzymes (*5*, *6*). A portion of the amino acids that form the interior walls of the ammonia tunnel were replaced by ones with bulkier side chains in an attempt to block the passage of ammonia. Some of these mutants displayed kinetic properties that were consistent with a model whereby the transport of ammonia is restricted. However, a crystal structure of the αG359F mutant revealed a structural reorganization of the protein backbone which apparently allows ammonia to escape from the molecular tunnel into the surrounding milieu (*7*). The mutation resulted in a change in the conformation of a random coil region between αGlu-355 and αAla-364, and the structural integrity of the ammonia tunnel was compromised.

The role of the comparable ammonia tunnel in phosphoribosylpyrophosphate amidotransferase (PRTase) was investigated by mutant enzymes which contain a leaky ammonia tunnel (*8*). The channeling efficiency of the mutant F334A was less than 1% of the wild-type levels, and the K_m of glutamine was increased 40-fold. This residue is located in a flexible loop (residues 326−350) which covers the ammonia tunnel in PRTase. Structural ordering of this flexible loop is necessary for the formation of the ammonia tunnel, which is initiated by the binding of substrates. The ammonia tunnel in PRTase is the only example known thus far which requires substrate binding to organize the structure of the molecular tunnel. Other enzymes recognized to translocate ammonia apparently contain a permanent molecular tunnel (*9*−*12*).

In the present study, the functional properties of the ammonia tunnel in CPS have been further investigated by the construction of leaky tunnel mutants, which contain a rationally designed hole in the ammonia tunnel by site-directed mutagenesis. The leaky ammonia tunnel mutants were intended to comprise an outlet for ammonia to exit before it reaches the subsequent active site. The primary objective of the present investigation is to provide further experimental support for the mechanism where the internally generated ammonia diffuses directly through the ammonia tunnel within CPS. This has been attempted by replacing selected amino acids within the walls of the ammonia tunnel with alanine in order to generate a hole in the ammonia tunnel that leads directly to the protein surface. These alterations are expected to impede the delivery of ammonia from the site of generation in the small subunit to the site of utilization in the large subunit.

MATERIALS AND METHODS

Materials. All chemicals and coupling enzymes were purchased from either Sigma or Aldrich, unless otherwise stated. Restriction enzymes were purchased from New England Biolabs, and *pfu* DNA polymerase was acquired from Promega. The gene for ornithine transcarbamoylase (OTCase) was a generous gift from the laboratory of Professor N. Allewell.

Bacterial Strains and Plasmids. Site-directed mutagenesis of CPS was performed as described previously (*13*, *14*). The *Escherichia coli* strains used for this study were RC50 (*car* A50, *thi*-1, *mal*A1, *xyl*-7, *rsp*L135, λ^r, λ^-, and *tsx*-237) and XL1-Blue. The RC50 strain used for protein expression was a generous gift from Dr. Carol J. Lusty. All plasmids used in this project were derived from pMS03 (*13*). Oligonucleotide synthesis and DNA sequencing reactions were performed by the Gene Technology Laboratory, Texas A&M University.

Construction of Mutant Plasmids. Site-directed mutagenesis was performed using the polymerase chain reaction and the overlap extension method of Ho et al. (*15*). All of the site-directed changes made to the wild-type CPS were

confirmed by DNA sequencing of the modified plasmids. Amplified DNA fragments containing the desired sequence changes for the construction of βQ262A, βR265A, and βN266A were introduced into pMS03 through the *Sac*II and *Bsiw*I restriction sites in the *car*B gene of CPS. The *Pflm*I and *Apa*I sites were used for the construction of P360A/H361A and D362A in the *car*A gene.

Expression and Purification of Mutant Proteins. The plasmids containing the *car*AB genes were transformed in the RC50 cell line of *E. coli* for expression of the wild-type and mutant forms of CPS. The wild type and mutant variants of CPS were purified as previously described (*16*). The mutants αD362A, βR265A, αD362A/βR265A, βQ262A/βR265A, βQ262A/βR265A/βN266A, αP360A/αH361A, and αP360A/αH361A/βR265A were expressed and purified to greater than 95% homogeneity, as judged by SDS−polyacrylamide gel electrophoresis.

Kinetic Measurements and Analysis. The rate of ADP formation was measured using a pyruvate kinase/lactate dehydrogenase coupling system (*16*). The reaction mixtures for the glutamine/ammonia-dependent assay contained 50 mM Hepes (pH 7.6), 20 mM $MgCl_2$, 100 mM KCl, 40 mM $KHCO_3$, 5.0 mM ATP, 10 mM ornithine, 1.0 mM phosphoenolpyruvate, 0.2 mM NADH, 20 units of pyruvate kinase, 30 units of lactate dehydrogenase, and varying amounts of glutamine or ammonium chloride. The rate of ATP synthesis was measured with a hexokinase/glucose-6-phosphate dehydrogenase coupling system (*13*). The assay solution for the ADP-dependent assay included 50 mM Hepes (pH 7.6), 15 mM $MgCl_2$, 100 mM KCl, 10 mM ornithine, 0.75 mM NAD, 0.04 mg/mL hexokinase, 10 mM glucose, 0.0016 mg/mL G6DPH, 2.0 mM carbamoyl phosphate, and varying amounts of ADP. The synthesis of carbamoyl phosphate was determined by measuring the rate of citrulline formation in a coupled assay containing ornithine transcarbamoylase and ornithine (*17*). The assay mixture contained 50 mM Hepes (pH 7.6), 20 mM $MgCl_2$, 100 mM KCl, 40 mM $KHCO_3$, 5.0 mM ATP, 10 mM ornithine, 12 units of OTCase, and 10 mM glutamine. The rate of glutamine hydrolysis was determined by coupling the formation of glutamate to the production of α-ketoglutarate with L-glutamate dehydrogenase and 3-acetylpyridine adenine dinucleotide (*16*). The reaction mixture contained 50 mM Hepes (pH 7.6), 20 mM $MgCl_2$, 100 mM KCl, 40 mM $KHCO_3$, 5.0 mM ATP, 10 mM ornithine, 1.0 mM APAD, 56 units of L-glutamate dehydrogenase, and varying amounts of glutamine.

The kinetic parameters were determined by fitting the experimental data to eq 5 using Sigma Plot, where k_{cat} is the

$$v/E_t = k_{cat}A/(K_m + A) \quad (5)$$

turnover number, K_m is the Michaelis constant, and A is the substrate concentration. The data for the enhancement of ATP hydrolysis in the presence of a nitrogen source were fitted to eq 6 (*18*), where V_0 is the initial enzyme velocity in the

$$v = V_0(K_a + \alpha I)/(K_a + I) \quad (6)$$

absence of a nitrogen source, I (ammonia or glutamine), K_a is the apparent activation constant, and α is the ratio of the velocities in the presence and absence of a nitrogen source. In this case, k_{cat} is expressed as $\alpha V_0/E_t$.

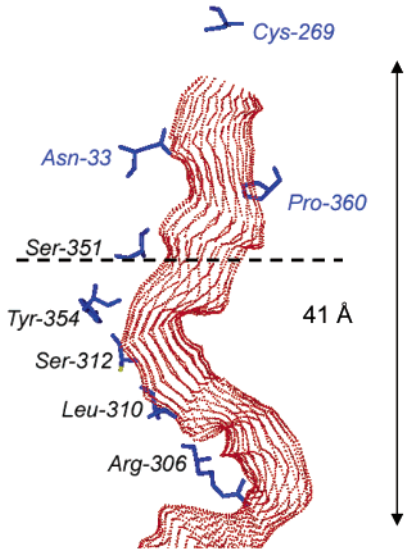

FIGURE 2: Molecular tunnel of CPS. Amino acids at the edges of the molecular tunnel from the small subunit and the large subunit are labeled in blue and black, respectively. The dashed line indicates the interface between the small and the large subunit.

RESULTS AND DISCUSSION

Amino acid residues surrounding the ammonia tunnel of CPS were mutated in an attempt to derail the passage of ammonia during the journey from the site of generation to the site of utilization by creating a shunt to the external protein surface. The three-dimensional crystal structure of CPS was dimensionally probed to determine which region of the protein is the most vulnerable for the creation of a detour for the migration of ammonia. The protein matrix of the enzyme was arbitrarily divided into 5 Å thick slices that were perpendicular to the long axis of the ammonia tunnel and extended from the active site cysteine in the small subunit to the termination of the ammonia tunnel within the large subunit. Each layer contained the amino acids indicated in Figure 2. The distance from the inside wall of the molecular tunnel to the outer protein surface was measured in each slab, and the distances varied from 8 to 22 Å. The shortest gap was measured from the α-carbons of Asp-362 and His-361 of the small subunit to the nearest point within the interior surface of the ammonia tunnel. This region of the protein is at the interface between the large and small subunits of CPS. The outer contour of the protein surface, relative to the position of the ammonia tunnel at the interface between the large and small subunits, is illustrated in Figure 3. An alternative view of the subunit interface is presented in Figure 4.

At the subunit interface, amino acid residues αPro-360, αIle-307, βGln-262, and βArg-265 comprise part of the interior wall of the ammonia tunnel. Located directly behind these residues are αHis-361, αAsp-362, βAsn-266, and βGlu-349, which constitute the exterior layer of the ammonia tunnel. βArg-265 interacts with αAsp-362 and βGlu-349 by ion pairing at distances of 3.0 and 2.7 Å, respectively. Residues αPro-360, αAsp-362, βGln-262, βArg-265, and βGlu-349 are highly conserved among other CPS enzymes, whereas βAsn-266 and αHis-361 are not. The long side chains of βGln-262, βArg-265, and βAsn-266 in the large subunit orient toward the small subunit and are therefore logical targets for the introduction of physical defects within

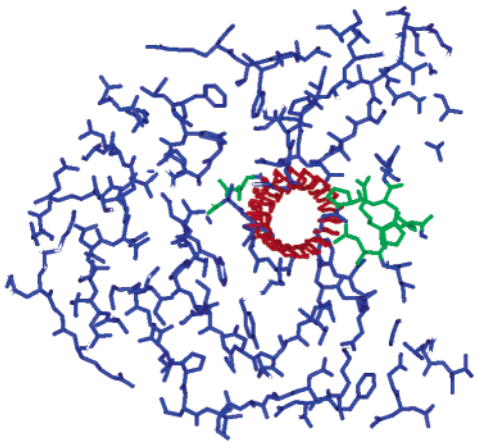

FIGURE 3: 5 Å cross-sectional layer of CPS at the interface between the large and small subunits viewed from the small subunit toward the large subunit. The positioning of the ammonia tunnel is shown in red. Amino acids αP360, αH361, βQ262, βR265, βN266, and βS351 are shown in green.

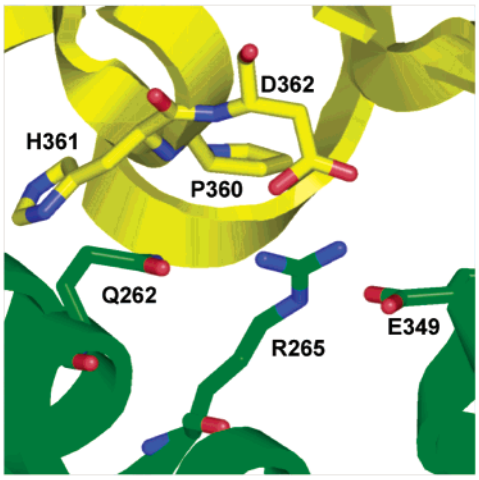

FIGURE 4: Positioning of amino acids targeted for mutagenesis. The amino acids from the small subunit are presented in yellow, and the amino acids from the large subunit are depicted in green.

the ammonia tunnel. The bulky side chains of these residues were mutated to alanine to create a series of mutants with the potential for the functional disruption of the ammonia tunnel. Residues that define the internal surface of the ammonia tunnel were selected first for modification, including αPro-360, βGln-262, and βArg-265. These residues are protected from the outside surface by αHis-361, αAsp-362, and βAsn-266. These capping residues were also considered for mutation in tandem with the interior wall residues to enable the formation of a direct link to the exterior protein surface.

The most vulnerable point for the disruption of the ammonia tunnel appears to be βArg-265. The side chain of this residue can be partially viewed from the outside of the protein and thus forms a single amino acid layer between the inside and outside of the ammonia tunnel. When βArg-265 was mutated to alanine, the kinetic constants for glutamine hydrolysis, ammonia-dependent ATPase, and carbamoyl phosphate synthesis are only modestly changed from the wild-type enzyme (Table 1). However, a 50-fold higher K_m for glutamine is observed in the glutamine-dependent hydrolysis of ATP and synthesis of carbamoyl phosphate. Since αAsp-362 interacts with βArg-265 through an ion pair (Figure 4), it was selected for mutation in an attempt to enlarge the putative outlet for ammonia in conjunction with the initial mutant, βR265A. The single mutant, αD362A, displays kinetic properties almost identical to those of the wild-type enzyme (Table 1). When this mutation was combined with βR265A, the double mutant behaves similarly to the single mutant βR265A. Therefore, the mutation of αAsp-362 does not affect significantly the catalytic function of the enzyme.

Residue βGln-262 is located next to βArg-265 in the three-dimensional framework of the enzyme and appeared to be an alternative site for mutation to enlarge the gap created by the initial mutation of βArg-265. However, the kinetic data of the double mutant, βQ262A/βR265A, are not significantly different from those of βR265A. Residue βAsn-266 is a second-sphere residue and is located directly behind βArg-265. However, βAsn-266 does not block completely the region covered by the side chain of βArg-265 in wild-type CPS. Therefore, the presence of this residue may account for the failure of the single mutant to form a pore large enough to allow for the leakage of ammonia. The residue βAsn-266 was mutated to alanine in conjunction with the previous mutations at βGln-262 and βArg-265 with the intention of generating a hole large enough to induce the seepage of ammonia. However, this design feature failed since the triple mutant βQ262A/βR265A/βN266A exhibited kinetic properties similar to those of the other βR265A mutants (Table 1).

Residue αPro-360 is one of the amino acids that constitute the interior wall of the ammonia tunnel, whereas αHis-361 is a second sphere residue. The double mutant, αP360A/αH361A, was constructed, and the kinetic properties were analyzed. The overall kinetic behavior closely resembles that of the wild-type enzyme, indicating that changes to these two residues by themselves do not affect the local structure of the protein significantly. These mutations were combined with the alanine alteration at βArg-265 and the triple mutant, αP360A/αH361A/βR265A, was constructed. The Michaelis constant for glutamine with this mutant is >300-fold higher than for the wild-type enzyme. The triple mutant αP360A/αH361A/βR265A exhibited no activation of ATP hydrolysis in the presence of glutamine up to 40 mM, whereas there was an 8.4-fold activation in k_{cat} in the presence of ammonia. The lack of activation of the glutamine-dependent ATPase reaction may have resulted from the reduced rate of attack on the carboxy phosphate intermediate due to the impeded delivery of ammonia. This mutant was also able to utilize external ammonia as a nitrogen source in the synthesis of carbamoyl phosphate. However, the mutant was not initially able to synthesize carbamoyl phosphate with glutamine at a comparable rate as an alternative source of nitrogen (Table 1). A reasonably high rate of glutaminase activity demonstrates that the function of the active site was not seriously affected by this mutation. Therefore, the largely attenuated rate of carbamoyl phosphate synthesis with glutamine as a nitrogen source must originate from a significant loss of ammonia during the delivery to the bicarbonate binding site through the ammonia tunnel. The elution profiles from size-exclusion chromatography during the purification of the wild-type CPS and all of the mutants constructed for this investigation were identical (data not shown). Therefore, the mutations created at the interface of the large and small

Table 1: Kinetic Parameters for the Glutaminase, ATPase, and Carbamoyl Phosphate Synthesis Reactions of the Wild-Type and Mutant Enzymes

	glutaminase[a]		NH_4^+-dependent ATPase[b]		Gln-dependent ATPase[b]		NH_4^+-dependent CP synthesis[c]		Gln-dependent CP synthesis[c]	
enzyme	k_{cat} (s^{-1})	K_m (mM)	k_{cat} (s^{-1})	K_m (mM)	k_{cat} (s^{-1})	K_m (mM)	k_{cat} (s^{-1})	K_m (mM)	k_{cat} (s^{-1})	K_m (mM)
WT	2.0 ± 0.1	0.14 ± 0.01	3.9 ± 0.1	130 ± 13	3.8 ± 0.1	0.10 ± 0.01	1.9 ± 0.1	130 ± 20	1.4 ± 0.1	0.11 ± 0.01
αD362A	2.1 ± 0.1	0.092 ± 0.02	9.5 ± 1.0	120 ± 17	4.7 ± 0.5	0.066 ± 0.007	3.8 ± 0.1	24 ± 3	2.4 ± 0.2	0.19 ± 0.04
βR265A	3.7 ± 0.1	0.36 ± 0.04	5.7 ± 0.3	41 ± 7	2.8 ± 0.1	6.4 ± 1.4	2.5 ± 0.3	26 ± 4	1.1 ± 0.04	7.6 ± 0.9
αD362A/βR265A	3.2 ± 0.1	0.38 ± 0.04	10.3 ± 0.3	55 ± 8	2.3 ± 0.1	5.5 ± 0.8	5.8 ± 0.1	59 ± 4	1.2 ± 0.1	7.8 ± 1.4
βQ262A/βR265A	2.6 ± 0.1	6.4 ± 0.9	5.0 ± 0.3	58 ± 11	2.9 ± 0.1	4.1 ± 0.6	3.6 ± 0.1	26 ± 3	1.0 ± 0.1	4.7 ± 0.8
βQ262A/βR265A/βN266A	1.7 ± 0.1	5.5 ± 0.8	6.7 ± 0.5	56 ± 11	1.9 ± 0.1	1.9 ± 0.2	ND[d]	ND	0.88 ± 0.05	14.9 ± 1.8
αP360A/αH361A	3.4 ± 0.1	$0.39 \pm .03$	4.0[e]	>300	6.0 ± 0.2	0.40 ± 0.05	2.0[e]	>300	2.3 ± 0.1	0.36 ± 0.04
αP360A/αH361A/βR265A	1.4[f]	>40	4.7 ± 0.3	59 ± 11	0.74[f]	>40	2.5 ± 0.1	12 ± 2	0.005[f]	>40

[a] The reaction mixture contained 50 mM Hepes (pH 7.6), 20 mM $MgCl_2$, 100 mM KCl, 40 mM $KHCO_3$, 5.0 mM ATP, 10 mM ornithine, 1.0 mM APAD, 56 units of L-glutamate dehydrogenase, and varying amounts of glutamine. [b] The reaction mixture contained 50 mM Hepes (pH 7.6), 20 mM $MgCl_2$, 100 mM KCl, 40 mM $KHCO_3$, 5.0 mM ATP, 10 mM ornithine, 1.0 mM phosphoenolpyruvate, 0.2 mM NADH, 20 units of pyruvate kinase, 30 units of lactate dehydrogenase, and varying amounts of glutamine or ammonium chloride. [c] The reaction mixture contained 50 mM Hepes (pH 7.6), 20 mM $MgCl_2$, 100 mM KCl, 40 mM $KHCO_3$, 5.0 mM ATP, 10 mM ornithine, 12 units of OTCase, and varying amounts of glutamine or ammonium chloride. [d] Not determined. [e] Specific activity measured at 300 mM NH_4Cl. [f] Specific activity measured at 40 mM glutamine.

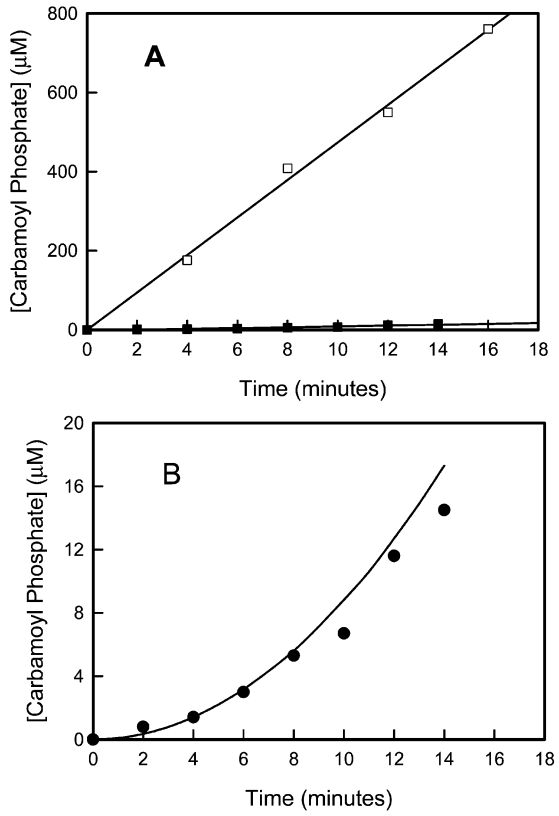

FIGURE 5: Time courses for the production of carbamoyl phosphate by αP360A/αH361A/βR265A from ammonium chloride (□) and glutamine (■) (panel A). Panel B displays the time course of the glutamine-dependent carbamoyl phosphate synthesis (●). The solid line in panel B is the calculated synthesis of carbamoyl-P from eq 7.

subunits did not cause the dissociation of the two subunits from one another.

The time courses for the synthesis of carbamoyl phosphate in the presence of ammonia and glutamine after the addition of the mutant αP360A/αH361A/βR265A are illustrated in Figure 5A. The enzyme works quite well with ammonia as a nitrogen source but not nearly at all with the addition of glutamine. Expansion of the vertical axis for the time course with glutamine reveals a lag phase for the limited formation of carbamoyl phosphate (Figure 5B). It is likely that the formation of carbamoyl phosphate with glutamine as a nitrogen source is due to the dissociation of free ammonia (produced from the hydrolysis of glutamine) into the medium and then reassociation with the protein. The rate of formation of ammonia can be calculated from the value of k_{cat} for the glutaminase assay (1.4 s^{-1} at 40 mM glutamine) and the total enzyme concentration (0.42 μM) to be 35 μM NH_3/min. Therefore, the concentration of ammonia will increase linearly from 0 to 490 μM after 14 min. Since the concentration of ammonia will not approach the Michaelis constant for NH_3, then k_{cat}/K_m (0.0125 μM^{-1} min^{-1}) can be used to estimate the rate of formation of carbamoyl phosphate from the concentration of free ammonia at any time t from eq 7.

$$[\text{carbamoyl phosphate}]_t = [NH_3]_t[k_{cat}/K_m][E_0]t/2 \quad (7)$$

The predicted time course for the formation of carbamoyl phosphate under these conditions is presented in Figure 5B. The production of carbamoyl phosphate accelerates as ammonia steadily accumulates in the bulk solution. The experimental time course for the glutamine-dependent carbamoyl phosphate synthesis fits well with the model where ammonia diffuses freely from the ammonia tunnel into the bulk solution and accumulates before it reenters the active site.

The channeling of an intermediate through a molecular tunnel will affect the cooperativity between sequential active sites. In the wild-type CPS, the reactions catalyzed at each active site are highly coupled with one another with an overall stoichiometry of 1:2:1 for the formation of glutamate, ADP, and carbamoyl phosphate, respectively. The stoichiometric coupling of product formation is likely modulated through conformational changes that are driven by binding and chemical events at the individual active sites. In CPS the conduits for the communication and signaling of information from one active site to another are unknown. It is likely that portions of the molecular tunnels that connect the active sites in CPS to one another are part of this signaling process. In the wild-type enzyme the k_{cat} for the glutaminase reaction is stimulated from a basal level of 0.0016 s^{-1} to 2.0 s^{-1} in the presence of ATP/HCO_3^-. With the αP360A/

Table 2: Relative Rates of Glutaminase, ATPase, and Carbamoyl Phosphate Synthesis of the Wild-Type and Mutant Enzymes

enzyme	glutamate formation	ADP formation	Gln-dependent CP synthesis
wild type	1.0	1.9	0.70
αD362A	1.0	2.2	1.1
βR265A	1.0	0.76	0.30
αD362A/βR265A	1.0	0.72	0.38
βQ262A/βR265A	1.0	1.1	0.38
βQ262A/βR265A/βN266A	1.0	1.1	0.52
αP360A/αH361A	1.0	1.8	0.68
αP360A/αH361A/βR265A	1.0	0.53	

αH361A/βR265A triple mutant, the basal level for glutamine hydrolysis is higher than for the wild-type enzyme (0.023 s^{-1}) and enhanced to >1.4 s^{-1} in the presence of ATP/HCO_3^-. These results indicate that the conduit for allosteric communication between the active site for glutamine hydrolysis and that for the phosphorylation of bicarbonate are largely intact. The observed ratios for the mutant enzymes are listed in Table 2, which illustrates the quantitative degree of coupling among the individual reactions at the three active sites. Except for αP360A/αH361A/βR265A, the other βR265A mutants exhibit ratios of approximately 1:1:0.5. Therefore, the hydrolysis of two glutamines is required for every carbamoyl phosphate that is ultimately formed. This result may be interpreted to indicate that only about 50% of the ammonia produced via the hydrolysis of glutamine in the small subunit is delivered to the carboxy phosphate binding site for the production of carbamate. However, with the mutant αP360A/αH361A/βR265A the reactions catalyzed by the active sites within the large and small subunits are completely uncoupled from one another.

For most of the mutants, the failure to divert all of the ammonia to the protein exterior may originate from a hole of insufficient diameter. The importance for the modification of βR265A is illustrated in Figure 6, which may be directly responsible for about 50% of the leakage-competent hole. Other mutations in the vicinity of βArg-265 were not effective in enlarging the hole, with the exception of αP360A/αH361A. Interestingly, the alteration at αPro-360 and αHis-361 alone was not sufficient to detect the leakage of ammonia. The structures of various mutants were simulated in order to support the generation of a pore via the replacement with alanine. Alteration at βArg-265A alone resulted in the formation of the hole which appears to be large enough to allow leakage of ammonia from the molecular tunnel. A surface rendering of the simulated structure of αP360A/αH361A/βR265A suggests that the additional modifications in the small subunit do not change the size of the hole significantly. The diameter of the hole is approximately 4 Å in Figure 6D. Other mutant enzymes, βQ262A/βR265A and βQ262A/βR265A/βN266A, however, display a larger sized hole, whereas the structures of αD362A and αP360A/αH361A do not exhibit any defect on the surface of the enzyme (data not shown).

On the basis of the kinetic data and the structural simulations, it appears that the mutations have caused further reorganization of the local structure. The βR265A mutation may have resulted in the collapse of the loop in the small subunit, which contains αPro-360, αHis-361, and αAsp-362, over the void in the large subunit induced by the alteration. The overall dimensions of the resulting hole may be smaller

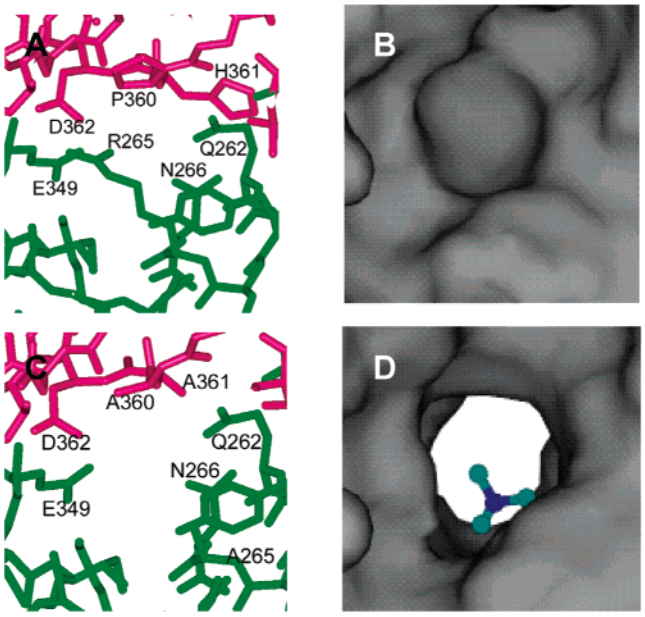

FIGURE 6: Structure of CPS around the mutation site as viewed from the inside of the ammonia tunnel toward the protein exterior. The wild-type enzyme is depicted in panels A and B. The representation of αP360A/αH361A/βR265A was generated by replacement of the indicated amino acids with alanine with the program Web Lab Viewer Pro (panels C and D). In panel D a molecule of ammonia is presented in a ball-and-stick format. The surface representations were constructed with the program SPOCK.

than what is required for the full diversion of ammonia to the exterior. Additional mutations at βQ262A and βN266A were not effective, probably for the same reason. However, modifications at αPro-360 and αHis-361 may have prevented the loop from collapsing or stabilized a structure with a gap of sufficient size. The alteration of these two amino acids by themselves was apparently not enough for the creation of a suitably sized pore.

A neighboring residue, αGly-359 in the small subunit, has been previously mutated to phenylalanine, which resulted in the formation of a structural reorganization within the ammonia tunnel (*7*). The kinetic properties of this mutant are similar to those of the mutant αP360A/αH361A/βR265A. The mutant αG359F was able to utilize ammonia as a nitrogen source but not glutamine in the synthesis of carbamoyl phosphate. However, the mutant was capable of hydrolyzing glutamine at a rate comparable to that of the wild-type enzyme, although the K_m for glutamine was elevated by at least 2 orders of magnitude. The mutant was not activated significantly by the hydrolysis of glutamine in the glutamine-dependent ATPase reaction but displayed a normal acceleration in the presence of ammonia. The X-ray crystal structure of αG359F revealed the structural reorganization of a loop which extends from αGlu-355 to αAla-364 (*7*). Since the kinetic constants of the double mutant αP360A/αH361A were essentially indistinguishable from those of the wild-type enzyme, it is not likely that the alterations at these amino acids induced a similar restructuring of the loop. The bulky side chain of phenylalanine that replaced αGly-359 could have caused a collision with neighboring residues, whereas substitutions with alanine at both αPro-360 and αHis-361 did not impose a significant structural stress on the surrounding residues in the double mutant enzyme.

ACKNOWLEDGMENT

We are indebted to Professor Hazel M. Holden for a critical reading of the manuscript and her efforts in the final preparation of Figures 1 and 4.

REFERENCES

1. Meister, A. (1989) Mechanism and Regulation of the Glutamine-dependent Carbamoyl Phosphate Synthetase of *Escherichia coli*, *Adv. Enzymol. Relat. Areas Mol. Biol. 62*, 315−374.
2. Anderson, P. M., and Meister, A. (1965) Evidence for an Activated Form of Carbon Dioxide in the Reaction Catalyzed by *Escherichia coli* Carbamoyl Phosphate Synthetase, *Biochemistry 4*, 2803−2809.
3. Thoden, J. B., Holden, H. M., Wesenberg, G., Raushel, F. M., and Rayment, I. (1997) Structure of Carbamoyl Phosphate Synthetase: A Journey of 96 Å from Substrate to Product, *Biochemistry 36*, 6305−6316.
4. Mullins, L. S., and Raushel, F. M. (1999) Channeling of Ammonia through the Intermolecular Tunnel Contained within Carbamoyl Phosphate Synthetase, *J. Am. Chem. Soc. 121*, 3803−3804.
5. Huang, X., and Raushel, F. M. (2000) An Engineered Blockage within the Ammonia Tunnel of Carbamoyl Phosphate Synthetase Prevents the Use of Glutamine as a Substrate but not Ammonia, *Biochemistry 39*, 3240−3247.
6. Huang, X., and Raushel F. M. (2000) Restricted Passage of Reaction Intermediates through the Ammonia Tunnel of Carbamoyl Phosphate Synthetase, *J. Biol. Chem. 275*, 26233−26240.
7. Thoden, J. B., Huang, X., Raushel, F. M., and Holden, H. M. (2002) Carbamoyl Phosphate Synthetase: Creation of an Escape Route for Ammonia, *J. Biol. Chem. 277*, 39722−39727.
8. Bera, A. K., Smith, J. L., and Zalkin, H. (2000) Dual Role for the Glutamine Phosphoribosylpyrophosphate Amidotransferase Ammonia Channel: Interdomain Signaling and Intermediate Channeling, *J. Biol. Chem. 275*, 7975−7979.
9. Larsen, T. M., Boehlein, S. K., Schuster, S. M., Richards, N. G., Thoden, J. B., Holden, H. M., and Rayment, I. (1999) Three-Dimensional Structure of *Escherichia coli* Asparagine Synthetase B: A Short Journey from Substrate to Product, *Biochemistry 38*, 16146−16157.
10. Binda, C., Bossi, R. T., Wakatsuki, S., Arzt, S., Coda, A., Curti, B., Vanoni, M. A., and Mattevi, A. (2000) Cross-talk and Ammonia Channeling between Active Centers in the Unexpected Domain Arrangement of Glutamate Synthase, *Struct. Folding Des. 8*, 1299−1308.
11. Chaudhuri, B. N., Lange, S. C., Myers, R. S., Chittur, S. V., Davisson, V. J., and Smith, J. L. (2001) Crystal Structure of Imidazole Glycerol Phosphate Synthase: A Tunnel through a $(\beta/\alpha)_8$ Barrel Joins Two Active Sites, *Structure 9*, 987−997.
12. Teplyakov, A., Obmolova, G., Badet, B., and Badet-Denisot, M. A. (2001) Channeling of Ammonia in Glucosamine-6-Phosphate Synthase, *J. Mol. Biol. 313*, 1093−1102.
13. Stapleton, M. A., Javid-Majd, F., Harmon, M. F., Hanks, B. A., Grahmann, J. L., Mullins, L. S., and Raushel, F. M. (1996) Role of Conserved Residues within the Carboxy Phosphate Domain of Carbamoyl Phosphate Synthetase, *Biochemistry 35*, 14532−14361.
14. Javid-Majd, F., Mullins, L. S., Raushel, F. M., and Stapleton, M. A. (2000) The Differentially Conserved Residues of Carbamoyl Phosphate Synthetase, *J. Biol. Chem. 275*, 5073−5080.
15. Ho, S. N., Hunt, H. D., Horton, R. M., Pullen, J. K., and Pease, L. R. (1989) Site-directed Mutagenesis by Overlap Extension Using the Polymerase Chain Reaction, *Gene 77*, 51−59.
16. Mareya, S. M., and Raushel, F. M. (1994) A Molecular Wedge for Triggering the Amidotransferase Activity of Carbamoyl Phosphate Synthetase, *Biochemistry 33*, 2945−2950.
17. Snodgrass, P. J., and Parry, D. J. (1969) The Kinetics of Serum Ornithine Carbamoyl Transferase, *J. Lab. Clin. Med. 73*, 940−950.
18. Cleland, W. W. (1970) Steady State Kinetics, *Enzymes (3rd Ed.) 2*, 1−65.

BI049945+